Statistical Characterization of Wireless Interference Signal Based On UWB Spectrum Sensing

Adeogun, Ramoni Ojekunle; Berardinelli, Gilberto; E. Mogensen, Preben; Rodriguez, Ignacio

Published in:
2020 IEEE 91st Vehicular Technology Conference (VTC2020-Spring)

DOI (link to publication from Publisher):
10.1109/VTC2020-Spring48590.2020.9128857

Publication date:
2020

Document Version
Accepted author manuscript, peer reviewed version

Statistical Characterization of Wireless Interference Signal Based On UWB Spectrum Sensing

Ramoni Adeogun*, Gilberto Berardinelli*, Preben Elgaard Mogensen*†, Ignacio Rodriguez*
*Wireless Communication Networks Section, Department of Electronic Systems, Aalborg University, Denmark
† Nokia Bell Labs, Aalborg, Denmark
E-mail:[ra, gb, pm, irl]@es.aau.dk

***Abstract*—Ultra-wideband (UWB) technology offers the potential for unparalleled support of short-range broadband communication over a multi-gigahertz spectrum and are expected to enable several applications with extreme requirements in future wireless networks. Enabling these systems in the unlicensed spectrum requires efficient co-existence management and adequate understanding of the characteristics and spatio-temporal dynamics of interference signals over the multi-GHz bandwidth. This paper investigates the suitability of Gaussian, Middleton canonical class A, symmetric alpha stable and Gaussian Mixture distributions for modelling radio frequency interference from systems in the UWB spectrum based on measurements. We evaluate the closeness of fit of the distributions to measured interference data and provide insights on the applicability of these models for characterizing interference in the UWB spectrum. Results show that the Gaussian Mixture distribution (GMD) yielded the best fit to the measured interference evaluated with Kullback-Leibler (KL) divergence below 0.05. Results also show that interference signals generated from the GMD agree closely with the measurements.**

***Index Terms*—UWB, Interference measurements, Gaussian mixture model, Interference modelling, statistical distributions, symmetric alpha stable distribution.**

I. Introduction

UWB transmission enables low power, short range communication over a large part of the radio spectrum from 3.1 GHz to 10.6 GHz, with tight restrictions in terms of power spectral density. The restrictions on transmission power limits the amount of interference from UWB devices to other co-existing users. However, UWB devices may be interfered by the large number of licensed and unlicensed systems such as WLAN, WiMAX, and satellite systems operating in the ultra-wide spectrum.

Recently, unlicensed spectrum is receiving attention as attractive option for the support of ultra-relaible and low latency communication [1], though it may suffer from regulatory limitations such as Listen Before Talk (LBT). It is therefore important to understand the behaviour of potential coexisting systems in such spectrum.

There has been considerable amount of research on interference from UWB devices to other co-exisiting systems such as WiFi, WIMAX and GPS, see e.g., [2] and the references therein. However, investigations on interference to UWB systems [3] has been mostly focused on performance evaluations and receiver processing techniques for specific UWB transmission technologies. For instance, approximations for multiuser interference in time hopping-UWB using Gaussian mixture distribution, Middleton class A noise and the Laplace distribution are investigated in [4] based on bit error rate performance simulations. In [5], results of a number of interference measurements at an indoor and outdoor location on the campus of Aalborg University, Denmark were presented. An analysis of the amplitude and inter-arrival time distributions were also presented. While it was shown that inter-arrival time between signal occurrence is predominantly exponential distributed, no model for amplitude and/or power distribution was investigated.

In this paper, we study the suitability of four statistical distributions viz: Gaussian, Middleton class A, symmetric alpha stable and Gaussian mixture distributions for characterizing interference signals over the entire UWB spectrum. While these models has been extensively studied for interference at different frequencies below 3 GHz, see e.g., [6]–[8], their suitability for interference signals at higher frequencies and possibility for a generic distribution that is able to model interference at different frequencies over a large spectrum remains an open problem. Based on the measurements in [5], we evaluate the goodness of fit of four statistical distributions to measured empirical probability distributions and give insights on their suitability for interference characterization. We further illustrate the accuracy of the distributions for interference modelling by sampling from the Gaussian mixture model and comparing with the measured signals.

The remaining part of this paper is organized as follows. The statistical distributions considered in the analysis are introduced in Section II. A discussion of the analysis as well as techniques for estimating parameters of the distributions from measurements is then presented in Section III. The results are discussed in Section IV. Finally, we draw conclusions in Section V.

II. Radio Frequency Interference Models

We present a brief overview of the interference models in this section. These distributions are chosen based on the expected differences in the characteristics of systems operating over the large bandwidth.

A. Gaussian Distribution

The Gaussian distribution represents each interference sample, x_k, as a realization of a random variable with probability

distribution function (pdf) defined as

$$f_{\mathrm{GD}}(x_k|\mu;\sigma^2) = \frac{1}{\sqrt{2\pi\sigma^2}} e^{-\frac{(x_k-\mu)^2}{2\sigma^2}}, \tag{1}$$

where μ and σ are the mean and standard deviation of the random variable, respectively. The Gaussian distribution is used extensively in the radio communication literature for several applications. However, it has been shown that interference signals are generally non-Gaussian [9].

B. Middleton Class A Model

Middleton class A model [9], [10] characterizes narrowband interference and is thus applicable when the receiver bandwidth is much larger than the interference spectrum as in the case of UWB systems interfered by signals from systems with relatively smaller bandwidth. The model defines an interference signal as the sum of a Gaussian and non-Gaussian component and the interference statistics is expressed as [9]

$$f_{\mathrm{MCA}}(x) = e^{-A} \sum_{n=0}^{\infty} \frac{A^n e^{-x^2/2\sigma_n^2}}{n!\sqrt{2\pi\sigma_n^2}}, \tag{2}$$

where the variance of the nth component, σ_n^2 is expressed as

$$\sigma_n^2 = \frac{\frac{n}{A} + \Sigma}{1 + \Sigma}. \tag{3}$$

The distribution in (2) is characterized by two parameters: an overlap/impulsive index, A, which is the product of the mean number of interfering signals arriving at the receiver per unit time and the mean duration of a typical interference signal, and a Gaussian factor, Σ, defined as the amplitude ratio of the Gaussian to non-Gaussian components.

C. Symmetric Alpha Stable Model

The Symmetric Alpha Stable (SαS) model [11] was proposed as an approximation to Middleton Class B model [9] for characterizing impulsive noise in cases where the noise (or interference) originates from a broadband system and has no Gaussian component. An interference sample, x_k, is said to be SαS distributed if its characteristic function is of the form [6], [11]:

$$\Phi(\omega) = e^{j\delta\omega - \gamma|\omega|^{\alpha}}, \tag{4}$$

where $\gamma(\gamma > 0)$ is the scale (or dispersion) parameter and δ is the localization parameter, which is equivalent to the median of the distribution. The parameter, α indicates the thickness of the distribution's tail and is often referred to as the characteristic exponent.

D. Gaussian Mixture Model

The Gaussian Mixture Model (GMM) represents each interference samples x_k as a realization of a random variable with probability distribution function (pdf) given by an N-components mixture of Gaussian pdfs [12]

$$f_{\mathrm{GMM}}(x_k|\boldsymbol{\Theta}) = \sum_{n=1}^{N} \lambda_n f_n(x_k|\mu_n;\sigma_n^2) \tag{5}$$

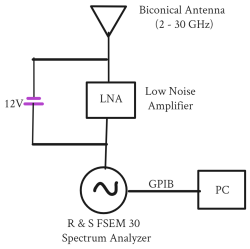

(a) Illustration of the set-up.

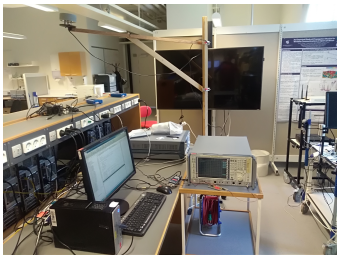

(b) Image from the Lab.

Fig. 1: Diagramatic illustration and picture of the measurement set-up.

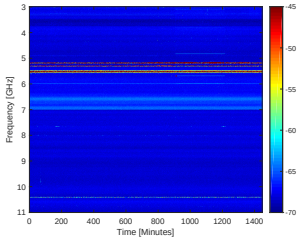

(a) WCN Lab.

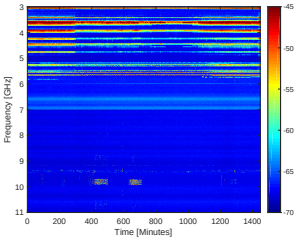

(b) FRB7 Roof Top.

Fig. 2: Spectrogram of UWB RFI obtained from measurements at WCN Lab and FRB7 roof top [5].

where $\boldsymbol{\Theta}$ is a vector of model parameters; $\boldsymbol{\Theta} = (\lambda_1, \cdots, \lambda_N, \sigma_1^2, \cdots, \sigma_N^2)$, λ_n are non-negative coefficients referred to as mixing probabilities, the sum of which is equal to unity, i.e., $\sum_{n=1}^{N} \lambda_n = 1$ and $f_n(x_k|\mu_n;\sigma_n^2)$ is the pdf of a Gaussian distribution with mean μ_n and variance, σ_n^2, defined as

$$f_n(x_k|\mu_n;\sigma_n^2) = \frac{1}{\sqrt{2\pi\sigma_n^2}} e^{-\frac{(x_k-\mu_n)^2}{2\sigma_n^2}}. \tag{6}$$

Thus, a GMM distributed interference sample has a pdf:

$$f_{\mathrm{GMM}}(x_k|\boldsymbol{\Theta}) = \sum_{n=1}^{N} \frac{\lambda_n}{\sqrt{2\pi\sigma_n^2}} e^{-\frac{(x_k-\mu_n)^2}{2\sigma_n^2}}. \tag{7}$$

III. UWB RFI Measurements and Data Fitting

In this section, we describe the radio frequency interference (RFI) measurements as well as procedure for estimating parameters of the distributions from the measured data.

A. Measurements

The RFI data used in this paper are from interference measurements in the 3 - 11 GHz band conducted at an indoor (i.e., Wireless Communication Networks laboratory) and outdoor (on the roof top of the FRB building) location on the premises of Aalborg University, Denmark [5]. The measurements were conducted using the system in Fig. 1 which comprises of; a $2\,\mathrm{GHz} - 30\,\mathrm{GHz}$ biconical antenna, a $2 - 18\,\mathrm{GHz}$ Low Noise Broadband Amplifier (LNBA) with $26\,\mathrm{dB}$ gain/3 dB noise figure, and a R & S FSEM 30 spectrum analyzer with

frequency range, 20 Hz - 26.5 GHz and resolution bandwidth (RBW) of 10 Hz - 10 MHz.

The datasets for the two locations contain 55000× 500 samples corresponding to 55000 consecutive sweep of the entire 8 GHz spectrum over a duration of 24 hours with resolution bandwidth (RBW) and video bandwidth (VBW) of 1 MHz.The maximum peak detector of the analyzer was used for all measurements and a total of 500 equally spaced discrete samples (i.e., bins) were recorded over the 8 GHz frequency span. Thus, the recorded spectrum analyzer measurements during each sweep correspond to the maximum power level within each 16 MHz bin from the start frequency (3 GHz) to the stop frequency (11 GHz). Detailed description of the measurements can be found in [5]. Measured spectrograms from the indoor and outdoor locations are shown in Fig. 2. The spectrograms show clear differences in signal activity at the two locations as well as across the spectrum.

B. Model Parameter Estimation

Empirical fitting of the interference models in Section II to measurements requires estimation of the models parameters. Parameter estimation for these models have been extensively investigated (see e.g., [6], [9]–[11], [13] and the references therein). For the MCA and GMM, Expectation Maximization (EM) [10], [12] algorithm have been shown to offer superior estimation performance over other methods and will be used in this study. We will estimate the parameters of the SαS model using the fast estimator in [14], which is based on the asymptotic behaviour of extreme-order statistics. For completeness, we summarize the estimation procedure for each of the models as follows.

1) Middleton Class A: Denoting the parameters of the MCA as $\boldsymbol{\theta} = [A, G]$, where $G = A\Sigma$, the EM method for MCA involves: [10]:

E-step: Evaluate the expected log-likelihood function, $Q(\boldsymbol{\theta}|\hat{\boldsymbol{\theta}}^p)$.

M-step: Determine $\boldsymbol{\theta} = \hat{\boldsymbol{\theta}}^{p+1}$ to maximize $Q(\boldsymbol{\theta}|\hat{\boldsymbol{\theta}}^p)$.

where $\hat{\boldsymbol{\theta}}^p$ denotes the parameter estimates at the pth iteration. A closed form expression for $Q(\boldsymbol{\theta}|\hat{\boldsymbol{\theta}}^p)$ is derived in [10].

2) Symmetric Alpha Stable: The estimators for the three parameters of the SαS are given as [14]

$$\begin{aligned}\hat{\delta} &= \text{median}[x_1, x_2, \cdots, x_K] \\ \hat{\alpha} &= \frac{\pi}{2\sqrt{6}}\left(\frac{1}{\sigma_{\min}} + \frac{1}{\sigma_{\max}}\right) \\ \hat{\gamma} &= \left\{\frac{\frac{1}{K}\sum_{k=1}^{K}(x_k - \hat{\delta})^v}{C(v,\hat{\alpha})}\right\}^{\hat{\alpha}/v},\end{aligned} \tag{8}$$

where $C(v, \hat{\alpha})$ is defined as

$$C(v,\hat{\alpha}) = \frac{\Gamma(1 - p/\hat{\alpha})}{\cos(\pi v/2)\Gamma(1 - v)} \tag{9}$$

In (8), $\sigma_{\min}$ and $\sigma_{\max}$ corresponds to the standard deviations of the minimum and maximum centered data segments obtained by dividing the interference samples into L non-overlapping subsets, respectively. Detailed discussion on the segmentation procedure can be found in [14].

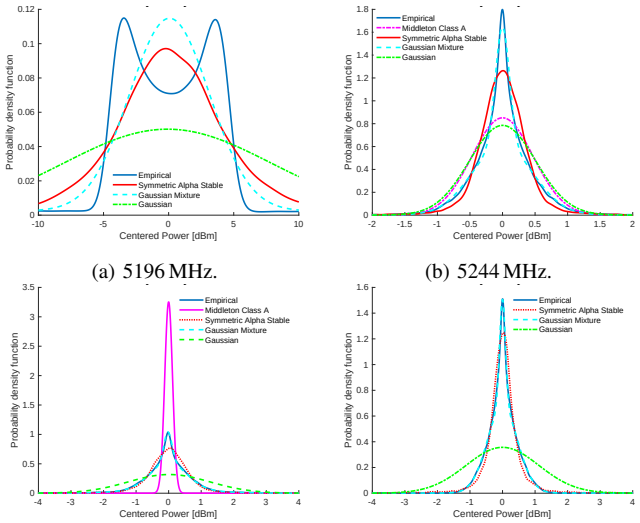

(a) 5196 MHz. (b) 5244 MHz.

(c) 5693 MHz. (d) 10406 MHz.

Fig. 3: Probability density function of selected measured RFI and fitted statistical models obtained from the indoor measurement.

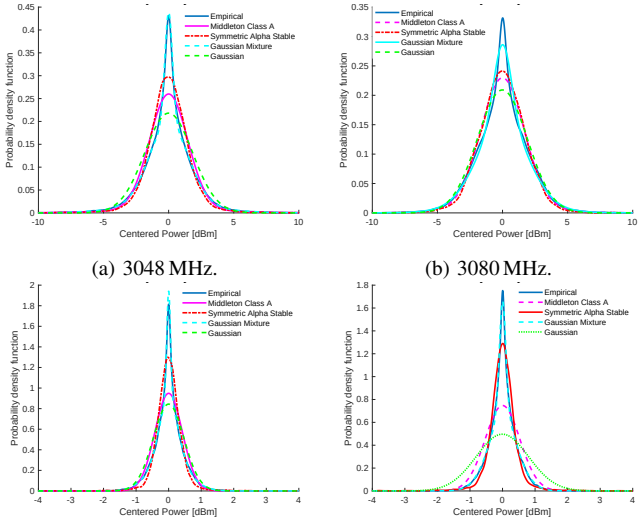

(a) 3048 MHz. (b) 3080 MHz.

(c) 9541 MHz. (d) 9910 MHz.

Fig. 4: Probability density function of selected measured RFI and fitted statistical models obtained from the outdoor measurement.

3) Gaussian Mixture Model: The steps in the EM estimator for the GMM are similar to those for the MCA with the parameter set; $\boldsymbol{\theta} = \{\lambda_n, \mu_n, \sigma_n^2\}_{n=1}^N$. Expressions for posterior probability distributions and the log-likelihood function are given in [12].

We will utilize the implementation of these estimation methods contained in an Interference Modeling and Mitigation MATLAB Toolbox [15] in this work.

IV. Results and Discussion

We now present results on the empirical fitting of the models in section II to the measured interference data. We used

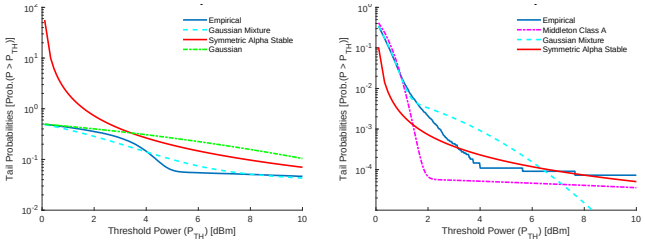

(a) 5196 MHz. (b) 5244 MHz.

(c) 5693 MHz. (d) 10406 MHz.

Fig. 5: Tail probabilities of measured RFI and fitted statistical models obtained from the indoor measurement.

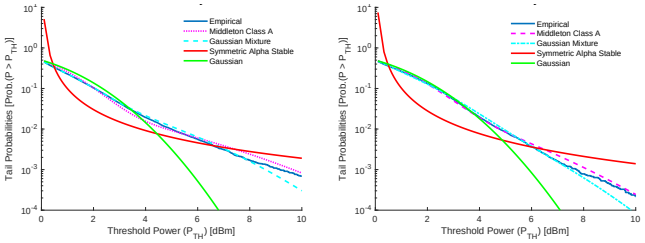

(a) 3048 MHz. (b) 3080 MHz.

(c) 9541 MHz. (d) 9910 MHz.

Fig. 6: Tail probabilities of measured RFI and fitted statistical models obtained from the outdoor measurement.

TABLE I: Estimated Kullback-Leibler divergence between empirical distribution and considered models.

Location	Freq.[MHz]	Kullback-Leibler Divergence			
		SαS	MCA	Gaussian	GMM
Indoor	5196	0.146	-	0.462	0.104
	5244	0.043	0.0951	0.130	0.008
	5324	0.056	-	0.707	0.007
	5533	0.207	-	0.683	0.128
	5693	0.032	2.219	0.314	0.046
	7665	0.047	0.058	0.131	0.011
	10406	0.149	-	0.619	0.031
Outdoor	3048	0.031	0.029	0.078	0.016
	3080	0.020	0.014	0.029	0.009
	9541	0.037	0.066	0.078	0.024
	9910	0.045	0.102	0.380	0.051

the Kullback-Leibler (KL) divergence (i.e., relative entropy between two probability distributions) to evaluate the similarities between the empirical probability distribution computed from measurements and distributions of each of the models. A KL divergence of zero indicates an exact match between the measured and fitted probability distributions. In the utilized toolbox, empirical probability distribution is computed using kernel smoothing density estimator [16]. Except where otherwise stated, the number of components for the GMM and MCA are 2 and 100, respectively. These values were heuristically selected and appear to provide reasonable fits to the measurements. However, in practical applications, methods for model order selection such as Akaike Information Criterion (AIC) and Bayesian Information Criterion (BIC) can be used to determine the best number of components for each distribution.

Fig. 3 shows the distribution functions of selected interference from the indoor measurements and the fitted models. The plots show that the Gaussian distribution does not fit any of the interference signals well. Except for the interference at 5196 MHz, probability distributions of the MCA, SαS and

TABLE II: Estimated parameters of two components GMM.

Location	Freq.[MHz]	Parameters					
		Mean		Variance		Probabilities	
Indoor	5196	0.066	-0.413	9.43	401.73	0.863	0.137
	5244	-0.016	0.001	2.245	0.129	0.055	0.945
	5324	0.0234	-0.013	95.77	0.439	0.055	0.945
	5533	0.019	-0.188	9.149	898.450	0.909	0.091
	5693	0.011	-0.252	0.354	30.630	0.960	0.040
	7665	0.001	0	0.477	0.062	0.300	0.700
	10406	0	0.015	0.175	35.670	0.97	0.030
Outdoor	3048	-0.018	0.011	7.041	0.943	0.387	0.613
	3080	0.009	-0.019	5.060	0.681	0.687	0.313
	9541	0	0.001	0.056	0.443	0.634	0.365
	9910	-0.0289	0	35.65	0.157	0.013	0.987

GMM exhibit some similarities with the measured distribution. The GMM is seen to yield the closest fit to all measured interference distributions. This agrees with the results in [4], where it was shown via simulations that the bit error rate of a TH-UWB systems with MUI GMM distributed agree closely with the actual BER.

Similar observations are made from Fig. 4, where we plot fitted distributions to interference signals in the outdoor measurement. However, Gaussian distribution fit to the signals at 3048 MHz and 3080 MHz appears much closer to the measured distributions when compared to the Gaussian fits in Fig. 3. Fig. 4 also shows that the SαS distribution is closer to the empirical distribution than the MCA for the signals at 3048 MHz, 3080 MHz, and 9541 MHz.

We present the tail probabilities (i.e., probability that the interference power deviates from its mean by a given amount or equivalently, the probability that the centered interference power exceeds a threshold, P_{TH}) for the indoor and outdoor measurements in Fig. 5 and Fig. 6, respectively. In Fig. 5, an exact match is seen between the tail probabilities of measured indoor signals and the GMM for interference sources at 5693 MHz in Fig. 4c and 10406 MHz in Fig. 4d. The tail probabilities of Gaussian and SαS distributions, differ significantly from the empirical probabilities. It is therefore

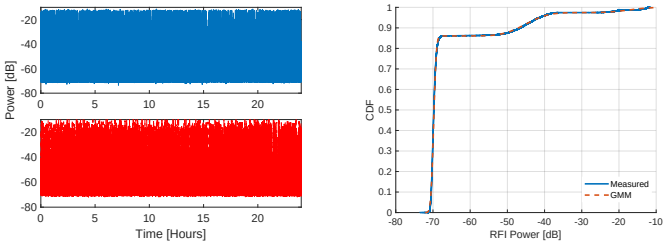

(a) Measured and Simulated RFI. (b) CDF

Fig. 7: Temporal variation and CDF of measured and simulated RFI from the 2 components GMM at 5196 MHz.

reasonable to infer that these interference signals can not be modelled using either Gaussian or SαS distributions. A plausible explanation for the difference between tail probabilities of the measured data and SαS distribution is that, the interfering signals can not be considered broadband relative to the large UWB spectrum. Similar agreement between the empirical tail probabilities obtained from the outdoor measurements and the GMM is seen in Fig. 6. In addition, the MCA distribution's fit shows good agreement to the empirical tail probability from the measurements. We show the KL divergence for all the distributions in Table I. The GMM and Gaussian distributions have the lowest and highest KL divergence for all interference sources in both measurements. This indicates that while Gaussian distribution is not suitable for interference modelling, most of the signals in the UWB can be approximated using the GMM.

The parameters of the two-components GMM distribution for the different interference signals is shown in Table II. These parameters, can for example be used to model realizations of interference at the measured frequency bands. The table shows that the model parameters differ for all sources except for the two interferers at 3048 MHz and 3080 MHz, which are spaced 32 MHz apart and may potentially originate from the same system(s).

Finally, we compare interference signals generated from the GMM distribution with measurements in Fig. 7 where we show the measured signal at 5196 MHz along with an example generated from the two components GMM. As seen in Fig. 7a, the simulated signal exhibits a high similarity with the measured interference indicating that GMM is a good statistical model for the interference at this frequency. This similarity is further shown in Fig. 7b where emprical CDF of the simulated signal matches that of the measured data very closely.

V. Summary and Conclusion

This paper presents the analysis of radio frequency interference measurements in the UWB spectrum between 3 GHz and 11 GHz. The suitability of Gaussian, MCA, SαS and GMM for modelling interference from different sources in the UWB has been evaluated based on measurements. Results show that interference signals in the UWB spectrum are not Gaussian distributed. MCA and SαS models provide reasonable fits to some of the interference signals. The GMM gives the best fit to all measurements and signals generated from this distribution agree closely with measurements. Study on temporal characteristics of these signals is the focus of our ongoing research.

References

[1] G. Berardinelli, N. H. Mahmood, I. Rodriguez, and P. Mogensen, "Beyond 5G Wireless IRT for Industry 4.0: Design Principles and Spectrum Aspects," in *2018 IEEE Globecom Workshops (GC Wkshps)*, Dec 2018, pp. 1–6.

[2] H.-J. Song, D.-K. Kim, M.-J. Kim, and H.-S. Lee, "A study of the interference measurement analysis between SDMB system and UWB wireless communication system," in *The 7th International Conference on Advanced Communication Technology, 2005, ICACT 2005.*, vol. 2, Feb 2005, pp. 1117–1120.

[3] S. V. Mir-Moghtadaei, A. Z. Nezhad, and A. Fotowat-Ahmady, "A new IR-UWB pulse to mitigate coexistence issues of UWB and narrowband systems," in *2013 21st Iranian Conference on Electrical Engineering (ICEE)*, May 2013, pp. 1–5.

[4] B. Hu and N. C. Beaulieu, "On characterizing multiple access interference in TH-UWB systems with impulsive noise models," in *2008 IEEE Radio and Wireless Symposium*, Jan 2008, pp. 879–882.

[5] R. Adeogun, G. Berardinelli, I. Rodriguez, P. E. Mogensen, and M. Razzaghpour, "Measurement and analysis of radio frequency interference in the uwb spectrum," in *IEEE 90th Vehicular Technology Conference (VTC2019-Fall)*, Sep. 2019, pp. 1–5.

[6] M. Nassar, K. Gulati, A. K. Sujeeth, N. Aghasadeghi, B. L. Evans, and K. R. Tinsley, "Mitigating near-field interference in laptop embedded wireless transceivers," in *IEEE International Conference on Acoustics, Speech and Signal Processing*, March 2008, pp. 1405–1408.

[7] K. Gulati, A. Chopra, R. W. Heath Jr., B. L. Evans, K. R. Tinsley, and X. E. Lin, "MIMO Receiver Design in the Presence of Radio Frequency Interference," in *IEEE GLOBECOM 2008 - 2008 IEEE Global Telecommunications Conference*, Nov 2008, pp. 1–5.

[8] M. Lauridsen, B. Vejlgaard, I. Z. Kovacs, H. Nguyen, and P. Mogensen, "Interference Measurements in the European 868 MHz ISM Band with Focus on LoRa and SigFox," in *2017 IEEE Wireless Communications and Networking Conference (WCNC)*, March 2017, pp. 1–6.

[9] D. Middleton, "Non-Gaussian noise models in signal processing for telecommunications: new methods an results for class A and class B noise models," *IEEE Transactions on Information Theory*, vol. 45, no. 4, pp. 1129–1149, May 1999.

[10] S. M. Zabin and H. V. Poor, "Efficient estimation of Class A noise parameters via the EM algorithm," *IEEE Transactions on Information Theory*, vol. 37, no. 1, pp. 60–72, Jan 1991.

[11] G. A. Tsihrintzis and C. L. Nikias, "Fast estimation of the parameters of alpha-stable impulsive interference," *IEEE Transactions on Signal Processing*, vol. 44, no. 6, pp. 1492–1503, June 1996.

[12] J. Bilmes, "A Gentle Tutorial of the EM Algorithm and its Application to Parameter Estimation for Gaussian Mixture and Hidden Markov Models," Int. Computer Science Institute, Tech. Rep., 1998.

[13] X. Dan, Z. Huimin, and Y. Yang, "Fast and efficient estimation of the symmetric alpha-stable impulsive signal or noise parameters," in *Proceedings of Third International Conference on Signal Processing (ICSP'96)*, vol. 1, Oct 1996, pp. 213–216.

[14] G. A. Tsihrintzis and C. L. Nikias, "Fast estimation of the parameters of alpha-stable impulsive interference using asymptotic extreme value theory," in *International Conference on Acoustics, Speech, and Signal Processing*, vol. 3, May 1995, pp. 1840–1843.

[15] K. Gulati, M. Nassar, A. Chopra, N. B. Okafor, M. DeYoung, N. Aghasadeghi, A. Sujeeth, and B. L. Evans, "UT Austin Interference Modeling and Mitigation Toolbox," online. [Online]. Available: http://users.ece.utexas.edu/~bevans/projects/rfi/software/index.html(accessed:03/04/2019)

[16] E. Parzen, "On Estimation of a Probability Density Function and Mode," *The Annals of Mathematical Statistics*, vol. 33, no. 3, pp. 1065–1076, 1962.